SMOKEBOT

Mobile Robots with Novel Environmental Sensors for Inspection of Disaster Sites with Low Visibility

Project start: January 1, 2015

Duration: 3.5 years

Due date: month 40 (April 2018)

Lead beneficiary: LUH

Dissemination Level: PUBLIC

Main Authors:

Paul Fritsche (LUH)

Version History:

0.1: Initial version, PF, March 2018
0.2: Corrected version, PF, April 2018

Contents

Abstract

This document is a description of the Navigation Sensor Fusion Toolkit within the scope of the Horizon 2020 project SmokeBot. SmokeBot's objective is to improve the application of mobile robots in disaster scenarios with low visibility conditions. The navigation sensor fusion toolkit includes new methods to fuse information from visible light based sensor and radar (3D LiDAR and data measurements from T1.1) in order to navigate robustly through environments that exceed controlled laboratory conditions.

This document includes experiments as well, which were necessary in order to find out about effects of smoke on LiDAR scanner, which are commonly used for SLAM and navigation. Based on the observed effects, three approaches for fusion LiDAR and radar were developed and implemented in ROS. After implementing our algorithms, we tested them in several experiments, which are presented in the last section of this document.

1. Introduction

LiDAR sensors are very popular for mapping and localisation with mobile robots, yet they cannot handle harsh environments, containing smoke, fog, dust etc.. On the other hand, radar sensors can overcome these situations, but they are not able to represent an environment in the same quality as a LiDAR due to their limited range and angular resolution. In the following document, we present the navigation sensor fusion toolkit, which is the basis for SLAM and navigation in environments with limited vision. Phillips et al. [1] already observed the effects of dust on Laserscanner. We observed the same behavior in case of smoke. In Fig. 1, we introduce the term “Type I” and “Type II” referring to a detection and absorption of LiDAR scans.

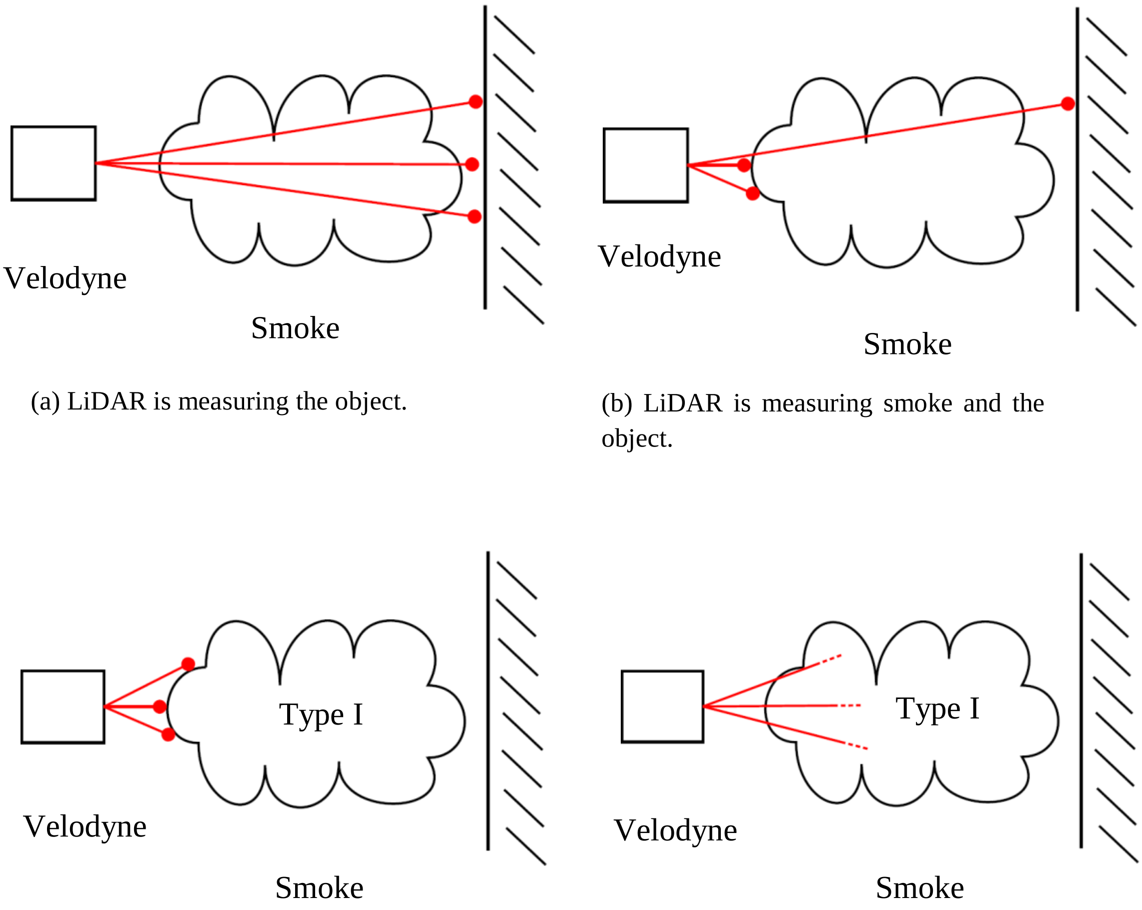

(a) LiDAR is measuring the object.

(b) LiDAR is measuring smoke and the object.

(c) LiDAR is measuring only smoke.

(d) LiDAR gets absorbed

Fig. 1 Smoke causes different effects on LiDAR scans

During our experiments, we observed basically two effects of smoke on LiDAR scanner, which are demonstrated in Fig. 2 and Fig. 3..

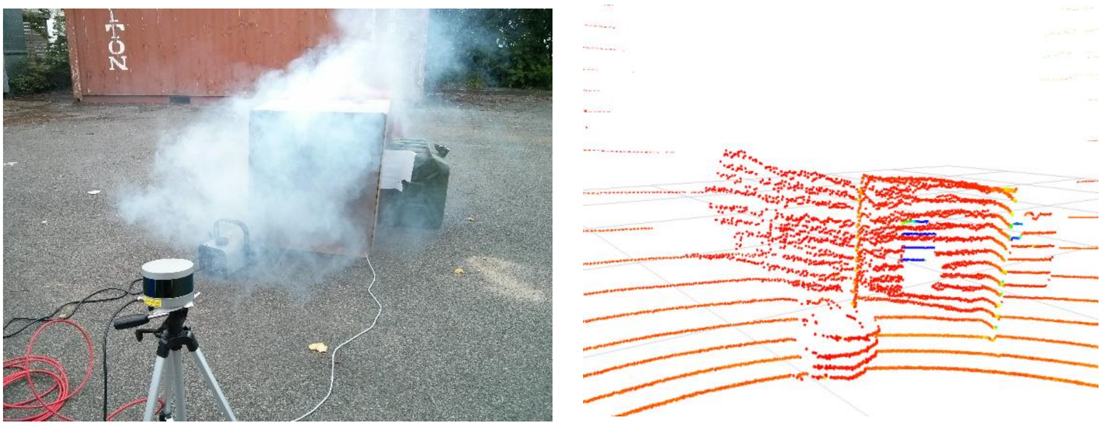

Fig. 2 The aerosol Type I effect is caused by detections of single smoke particles. Left: static experiment involving a fog machine. Right: The 3D LiDAR detects the fog, which occludes the scene consequently.

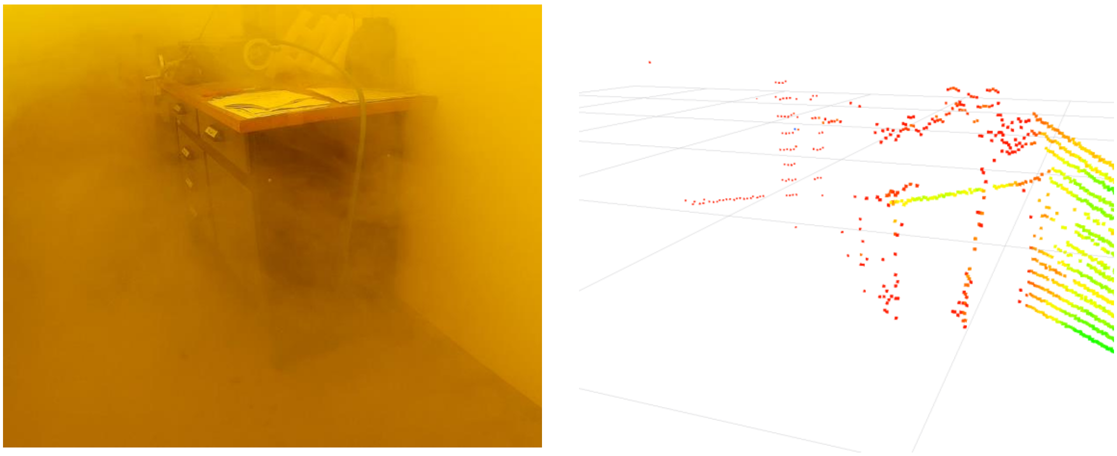

Fig. 3 The aerosol Type II effect is caused by absorption of single laser beams due to smoke particles. Left: Scene with very dense fog. Right: The 3D LiDAR is missing measurements due to the absorption.

Sensor fusion aims to combine sensor data to get more precise or abstract information. Brooks and Iyengar [2] classify sensor fusion into complementary, competing, cooperative, and independent fusions. Relevant for our scan fusion approach is the complementary and competing sensor fusion. Fusing different range sensors, complementary areas exist due to different maximum scan ranges. Competing sensor fusion takes place in overlapping scan fields, where it is necessary to decide to either rely on LiDAR, Radar or fuse both sensors. This decision is made automatically for every scan point by our fusion strategies.

Our scan fusion combines radar and LiDAR-scans. As we introduced in [3], the MPR produces a 2D scan, similar to a LiDAR, containing the strongest or nearest reflectors from every FFT spectrum of every single measurement. Furthermore, we presented with FHR details and specs regarding the MPR in [3]. The proposed scan fusion algorithms work with MPR and 2D or 3D LiDAR scans. The fusion with 2D LiDAR scanner is straightforward. A 3D scanner can enhance the fusion result through additional information. In the case of 3D LiDAR data, we extract virtual 2D scans [4]. The key idea of virtual 2D scans is the extraction of points inside a 3D scan that are suitable for mapping and localization and their projection into two-dimensional space. For most indoor environments, these points come from static objects like walls and other plane geometries. We extract wall measurements by choosing the furthest point of every vertical row of 3D measurements inside a scan. Furthermore, we verify plane geometries through horizontal line segmentation via RANSAC inside the LiDAR scans. If we find line segments inside the LIDAR scans, we can assume already that they do not come from aerosol detections, since smoke always appears in an unstructured fashion in the scan data.

Regarding our sensor setup (MPR and Velodyne VLP-16), LiDAR has a larger maximum scan range than radar, although the maximum ranges are not constant. It depends on the reflectivity of the objects inside the scene. For our approach, both sensors are aligned to the same center of rotation close to each other, as it is demonstrated in Fig. 4 Consequently, every range measurement of the LiDAR R_{LIDAR} has a corresponding range measurement of the radar R_{Radar}. A sensor fusion can only be performed in an overlapping scan field, which is defined by the radius R_{F} and gets calculated for every fusion cycle. It depends on the average range of a radar scan $R_{\text{Radar},\emptyset}$, the maximum range measurement of a radar scan $R_{\text{Radar,max}}$ and the parameter β = [0..1].

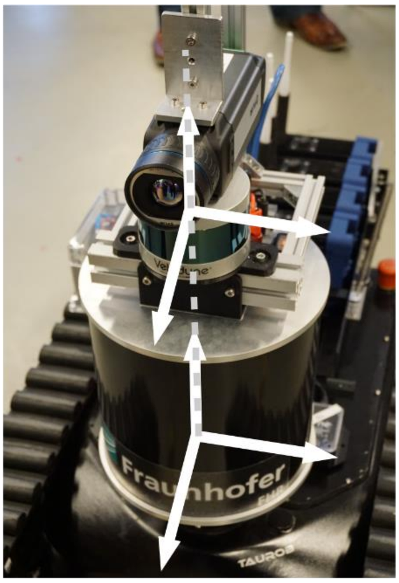

Fig. 4 Sensor setup for the navigation sensor fusion

$$R_{\mathrm{F}} = R_{\mathrm{Radar},\varnothing} + \beta\left(R_{\mathrm{Radar,max}} - R_{\mathrm{Radar},\varnothing}\right)$$

The following section describes the navigation sensor fusion tool kit, which can handle the Type I and II effect by integrating radar data.

2. How to work with the Navigation Sensor Fusion

The navigation sensor fusion consists of two ROS packages, which can be seen in Fig. 5. The packages have been tested in ROS versions Indigo and Kinetic.

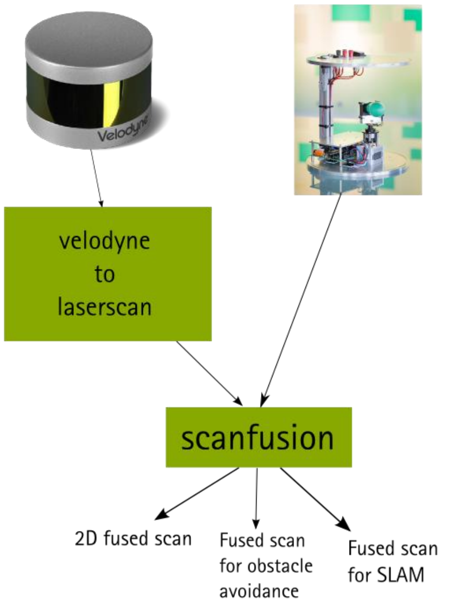

Fig. 5 The navigation sensor fusion toolkit

The following sections describe how to install, start and tune the fusion.

2.1 Install the package

Before building the packages, be sure that the following ROS packages are installed:

- pcl_ros
- velodyne_pointcloud
- grid_map

Then, clone velodyne_to_laserscan and scan_fusion to your workspace and built once via:

```
catkin_make -DCMAKE_BUILD_TYPE=Release
```

Quickstart:

To start the scan fusion, the MPR and Velodyne VLP need to be running.

```
roslaunch scan_fusion scan_fusion.launch
```

2.2 velodyne_to_laserscan package

This package generates 2D scans according to the idea of virtual 2D scans. It generates four 2D scans as sensor_msgs::LaserScan. The /laser_scan_with_ransac_2D_cut is based on a ring of the Velodyne VLP-16. The /laser_scan_with_ransac is suitable for SLAM, since it contains mainly walls and other static structure of the environment. Obstacles of a scene and walls appear in the /laser_scan_obstacles scan. Obstacles without walls are stored in /laser_scan_obstacles_without_walls.

```
rosrun velodyne_to_laserscan pointcloud_to_laserscan_with_ransac_node
```

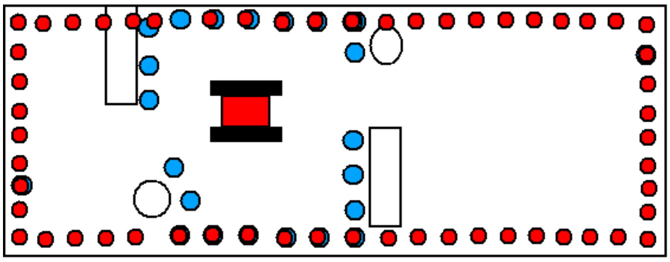

Fig. 6 laserscan_with_ransac (red) and laser_scan_obstacles (blue)

<u>Subscriber</u>

/velodyne_points (sensor_msgs::PointCloud2)

<u>Publisher</u>

/laser_scan_with_ransac_2D_cut (sensor_msgs::LaserScan, 2D laserscan based on a single ring of the Velodyne VLP16)

/laser_scan_with_ransac (sensor_msgs::LaserScan, 2D laserscan via virtual 2D scan method for SLAM)

/laser_scan_obstacles (sensor_msgs::LaserScan, 2D laserscan via virtual 2D scan method for obstacle avoidance)

/laser_scan_obstacles_without_walls (sensor_msgs::LaserScan, 2D laserscan via virtual 2D scan method for obstacle avoidance, without walls)

Dynamic Parameters:

RANSAC Paramters:

planar_points: Minimum number of points on a line segmentation

maxIterations: Maximum number of iteration for line segmentation

distanceThreshold: Distance of points to be considered on the line

nr_points_factor: stop searching for lines after this rate

Environment parameter with respect to the velodyne frame:

object_height_max: Maximum object height to include into /laser_scan_obstacles

object_height_min: Minimum object height to include into /laser_scan_obstacles

max_point_range: Maximum point distance to include into /laser_scan_obstacles

room_height_max: Maximum height of the scene (for example roof)

room_height_min: Minimum height of the scene (for example floor)

Size of the scans

scan_size_param: Number of point inside the scans

2.3 scan_fusion package

The scan_fusion merges 2D LiDAR and 2D MPR scans in order to overcome the Type I and II effect problem. The fused scan has the same size as the LiDAR scan.

```
rosrun scan_fusion scan_fusion
```

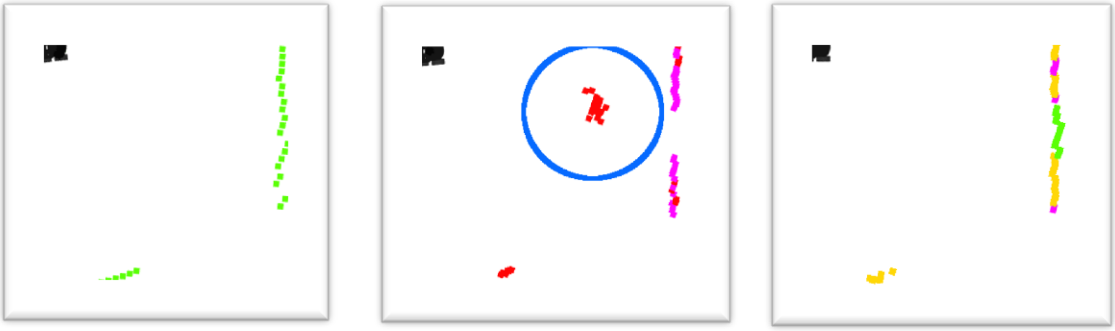

(a) MPR scan

(b) LiDAR scan (Type I Effect inside blue circle)

(c) Fused scan

Fig. 7 Three snapshots from MPR-, LiDAR- and fused scan at the same moment. The scanfusion handles the Type I Effect

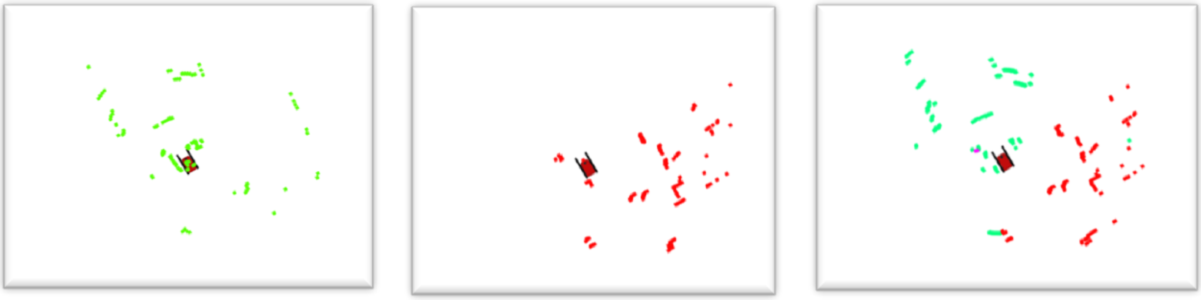

(a) MPR scan

(b) LiDAR scan (Type II Effect)

(c) Fused scan

Fig. 8 Three snapshots from MPR-, LiDAR- and fused scan at the same moment. The scanfusion handles the Type II Effect

Subscriber

/mpr_scan (sensor_msgs::LaserScan)

/laser_scan_with_ransac (sensor_msgs::LaserScan)

/laser_scan_obstacles (sensor_msgs::LaserScan)

/laser_scan_with_ransac_2D_cut (sensor_msgs::LaserScan)

Publisher

/mpr_scan_fixed (sensor_msgs::LaserScan,

the angle.min and angle.max is not constant inside the mpr_scan topic.

For example gmapping wont work with it. Therefore, I fixed it to a

constant value in the mpr_scan_fixed scan.)

/fused_scan_2D (sensor_msgs::LaserScan, fused scan between laser_scan_with_ransac_2D_cut and mpr_scan)

/fused_scan_obstacles (sensor_msgs::LaserScan, fused scan between laser_scan_obstacles and mpr_scan)

/fused_scan_slam (sensor_msgs::LaserScan, fused scan between laser_scan_with_ransac and mpr_scan)

Dynamic Parameters:

Rotation_calibration (The calibration between MPR and Velodyne can be tuned here. The velodyne frame is fixed and the MPR scan can be rotated)

MPR_Version (There is an offset difference regarding ORU's und LUH's MPR version. Therefore, it is necessary to choose the version)

Fusion_Algorithm (Select Heuristic, Model or GridBased Fusion)

Heuristic Fusion

dF (Heuristic fusion band)

alpha (max fusion range)

Model Fusion

p (defines fusion band similar to dF)

alpha (max fusion range)

GridBased Fusion

gridbasedFusion_weight (Weight the LiDAR or Radar 0...100)

res (Resolution of the gridmap which is used to fuse the sensor data)

3. Theory behind the fusion approaches

3.1 Heuristic Approach

The heuristic fusion approach is based on several conditions, which follow observations from experiments involving smoke.

$$S_{\text{Fusion}} = \begin{cases} R_{\text{LiDAR}}, \text{if} & \bullet\ \ |R_{\text{LiDAR}} - R_{\text{Radar}}| > d_{\text{F}} \\ & \quad \cap R_{\text{LiDAR}} \in \text{Line} \\ & \bullet\ \ R_{\text{LiDAR}} > R_{\text{F}} \\ & \quad \cap R_{\text{LiDAR}} \neq \text{inf} \\ & \bullet\ \ R_{\text{LiDAR}} - R_{\text{Radar}} > d_{\text{F}} \\ & \quad \cap R_{\text{LiDAR}} < R_{\text{F}} \\ R_{\text{Radar}}, \text{if} & \bullet\ \ R_{\text{LiDAR}} - R_{\text{Radar}} < -d_{\text{F}} \\ & \quad \cap R_{\text{LiDAR}} < R_{\text{F}} \quad \text{(Type I)} \\ & \bullet\ \ R_{\text{LiDAR}} = \text{inf} \\ & \quad \cap R_{\text{Radar}} \neq \text{inf} \quad \text{(Type II)} \\ R_{\text{Fusion}}, \text{if} & \bullet\ \ |R_{\text{LiDAR}} - R_{\text{Radar}}| < d_{\text{F}}. \end{cases}$$

If corresponding points from LiDAR and radar are inside the fusion range R_F having a distance larger than d_F to each other, then it is likely that the LiDAR beam hits an aerosol particle, if the LiDAR measurement is smaller than the radar measurement. Outside the fusion range R_F, only the sensor with larger maximum scan range can contribute to the fused scan. As already mentioned, we apply a line detection on the LiDAR scan. If a LiDAR point is on a line, then it is most likely not detecting an aerosol cloud and can be used for S_{Fusion}.

3.2 Model Approach

The model based approach calculates a fused scan S_{Fusion} via a function $f(i)$ for ever fusion cycle.

$$S_{Fusion}[i] = f(i) \cdot S_{LiDAR}[i] + (1 - f(i)) \cdot S^{*}_{Radar}[i]$$

The function $f(i)$ consists of several sigmoid functions. The behavior of the model-based approach is very similar to the heuristic approach.

$$f(i) = ((sig_{TypI} \cdot sig_{TypII} \cdot (1 - sig_{RF}) + sig_{RF}) \cdot (1 - sig_{FS})) + sig_{FS}$$

In order to calculate single sigmoid functions, the difference ΔS between LiDAR-scan and radar-scan is used. Since the size of the LiDAR-scan S_{LiDAR} can be selected via the parameter **scan_size_param** and the MPR scan has a constant size of 200 measurements, the size of the MPR-scan has to be adapted (S^{*}_{Radar}).

$$\Delta S = S_{LiDAR} - S^{*}_{Radar}$$

Equivalent to the heuristic approach, the Type I and Type II effect is handled via sig_{TypeI} and sig_{TypeII}. The parameter p defines a fusion band, where LiDAR and Radar range measurements get weighted. The parameter b should be set with a high value (>100) in order to have a behavior similar to a Sign function.

$$sig_{TypI}(i) = \frac{1}{1 + e^{-p\Delta S[i]}}$$

$$sig_{TypII}(i) = \frac{1}{1 + e^{b(\Delta S[i] - c)}}$$

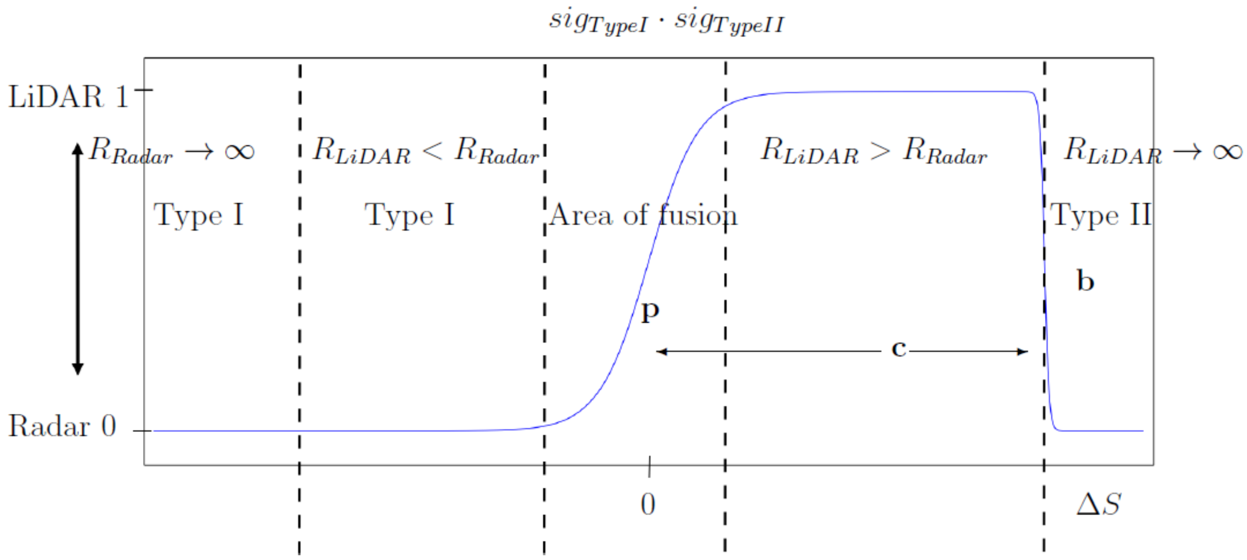

Fig. 9 Handling the the Type I and Type II effect can be realized with two sigmoid functions.

Since the Velodyne VLP 16 ha a larger maximum scan range then the MPR, only LiDAR can contribute outside the overlapping scan fields.

$$sig_{R_F} = \frac{1}{1 + e^{d(S_{LiDAR}[n]+R_F)}}$$

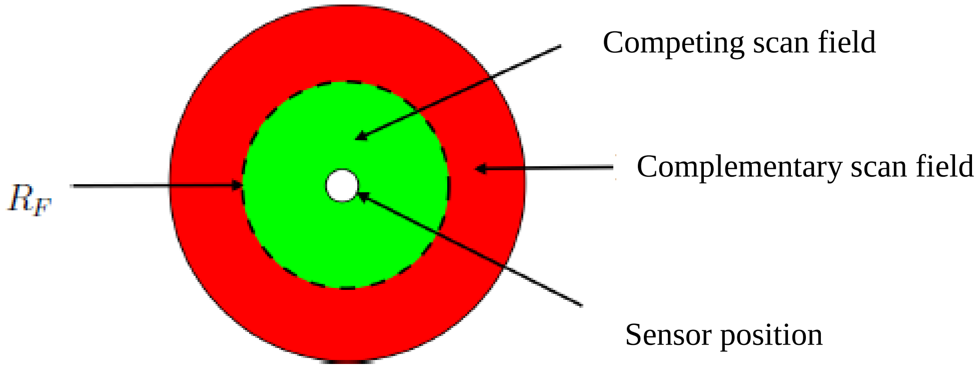

Fig. 10 Overlapping scan fields result in a complementary and competing scan field

The RANSAC line segmentation gives already a prediction for the presence of free sight (FS).

$$sig_{FS}(i) = \frac{1}{1 + e^{-a \cdot \Delta S[i]}}$$

3.3. Virtual Sensor Approach

The virtual sensor approach discretizes the scan in a gridmap and fuses them according to a weight a. Afterwards a raycast is determined for every virtual beam by using the maximum values, which gets hit by every virtual beam. This approach has a higher CPU consumption then the heuristic and model-based approaches.

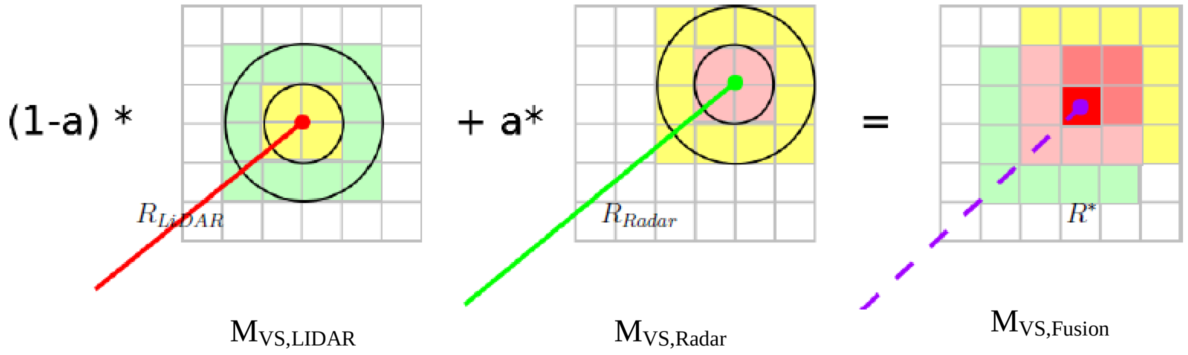

Fig. 11 Theory of operation of the Virtual Sensor. The **gridbasedFusion_weight (a)** parameter defines the strength of a LiDAR or Radar measurement regarding the fusion. The **res** parameter defines the resolution of the grids.

$$M_{VS,Fusion} = (100 - a) \cdot M_{VS,LiDAR} + a \cdot M_{VS,Radar} \qquad a = [0 \dots 100]$$

In order to handle the Type I effect, the weight a has to be larger than 50.

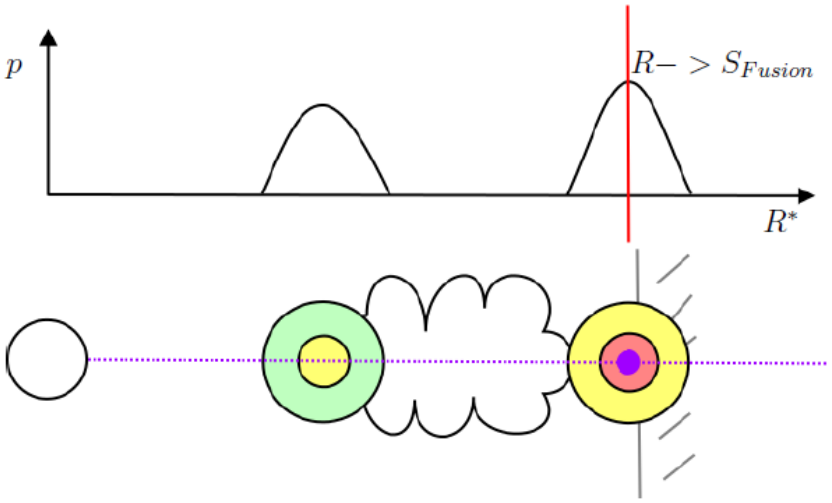

Fig. 12 Handling of the Type I effect due to stronger weight on $M_{VS,Radar}$

4. Experiments

4.1 The influence of the navigation sensor fusion on SLAM

Before performing our main experiment, we wanted to see if it is possible to integrate MPR scans into scan registration based SLAM approaches, because previous studies indicate that due to most radar scanners' bad accuracy and resolution, the focus has been on feature based SLAM approaches. Therefore, we drove up and down a corridor in a university building with a Pioneer platform and recorded radar and LiDAR data. We mounted the MPR and the Velodyne VLP-16 on a differential drive robot, similar to the taurob tracker, and collected data from an indoor environment. The scene can be seen in Fig. 13.

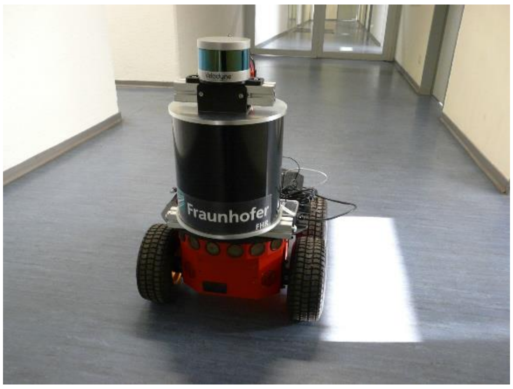

Fig. 13 Indoor environment without smoke

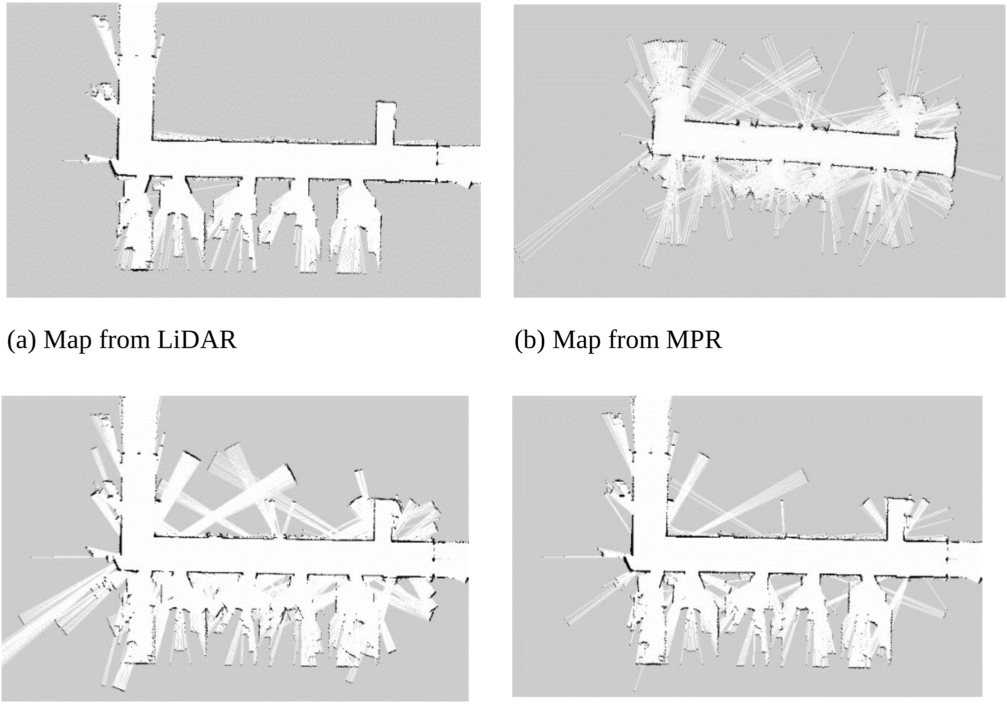

(a) Map from LiDAR

(b) Map from MPR

(c) Map from sensor fusion without RANSAC

(d) Map from sensor fusion with RANSAC

Fig. 14 SLAM result depends on sensors and parameters of sensor fusion

As shown in Fig. 14(d), outliers inside the resulting map can be diminished via RANSAC filtering, although it is not possible to erase them completely. Consequently, if an environment does not contain any smoke, fog or dust, then a radar scanner has no advantageous over a LiDAR scanner. Our fusion method enhances the resulting map under normal conditions. Since we are not able to suppress all outliers, the map from fused sensor data still contains more spikes than the pure LiDAR map. Nevertheless, a RANSAC line extraction as a pro prediction for a low visibility leads to less radar points inside the fused scans. The amount of radar points A_{Radar} inside the fused scan S_{Fusion} can be calculated as follows:

$$A_{Radar} = \frac{n_{Radar}}{n_{Radar} + n_{LiDAR} + n_{Fused}}$$

The amount of radar points over the time of the experiment is depicted in Fig. 15.

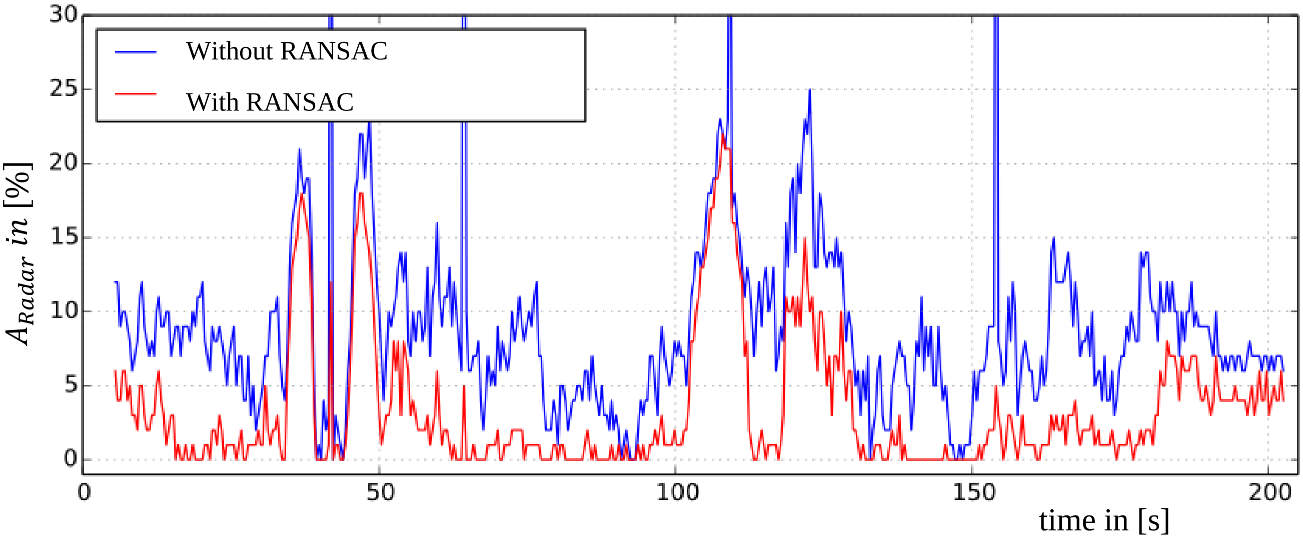

Fig. 15 Amount of radar in S_{Fusion} can be reduced with RANSAC filtering

4.2 Experiments involving the Type I Effect

We performed an experiment involving fog in order to see the effect of aerosols on LiDAR and Radar. We used a simple Eurolite fog machine (see Fig. 16).

The aim of the experiment is counting the number of detected fog particles inside the area A_C over the time of the whole experiment. In Fig 17 it can be seen, that for example LiDAR points get detected inside the area A_C (red circle). The setup is demonstrated in Fig. 18.

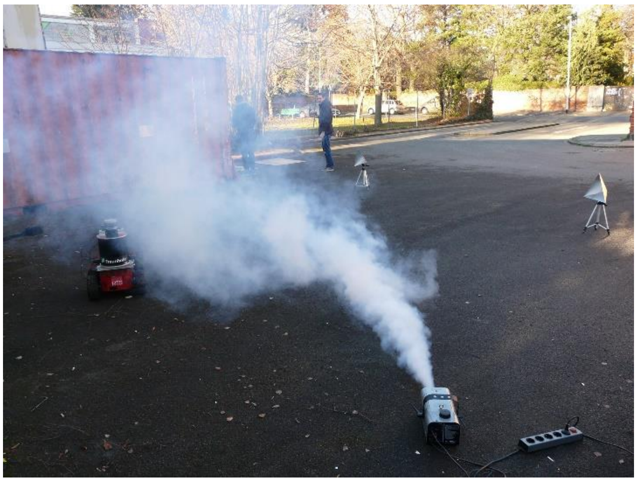

Fig. 16 Robotic Platform with MPR and Velodyne VLP-16 in a smoke scenario.

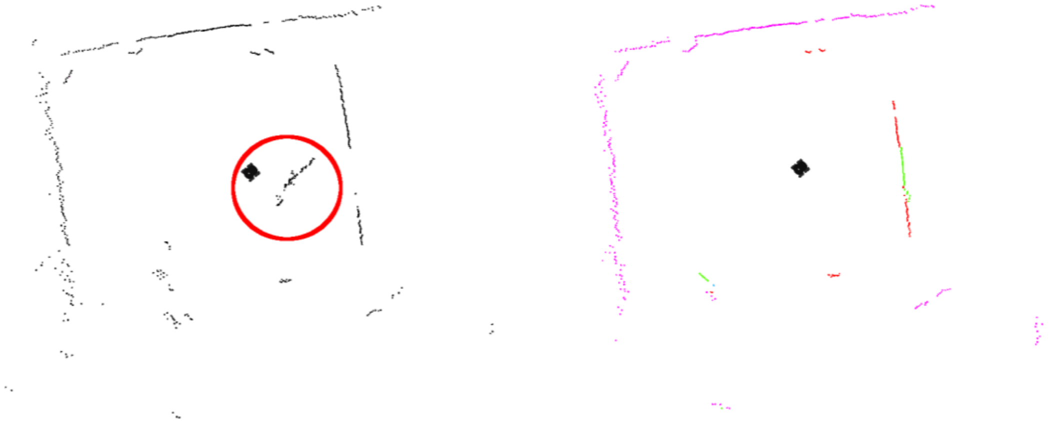

Fig. 17: Left: The robot and detected smoke is visible (inside the red circle): The LiDAR reports smoke in the same way as an obstacle. Right: The fusion algorithm combines Velodyne VLP16 and MPR measurements and replaces LiDAR points that are affected by smoke with radar points (green), which combines the advantage of both sensors – the higher accuracy of the LiDAR and radar measurements that are not disturbed by smoke.

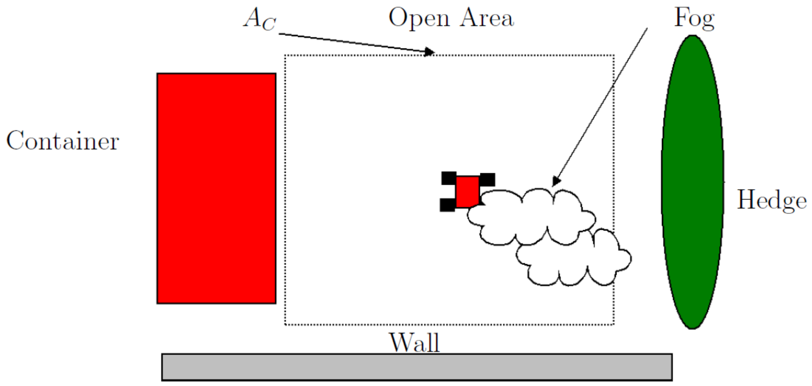

Fig. 18 Setup of the experiment

The total amount of detected aerosol particles from the LiDAR S_{LiDAR} (**/laser_scan_with_ransac_2D_cut**) is 7157. In Fig. 19, it can be seen that the behavior of the model based and heuristic approach is very similar regarding the handling of the Type I effect and that planar_points = 300 is a good setting for the 2D LiDAR 2D Radar fusion (**/fused_scan_2D**). It can be seen as well that the virtual sensor approach does not handle the Type I effect as well as the other two approaches. This is because the virtual sensor approach cannot handle smoke in front open areas.

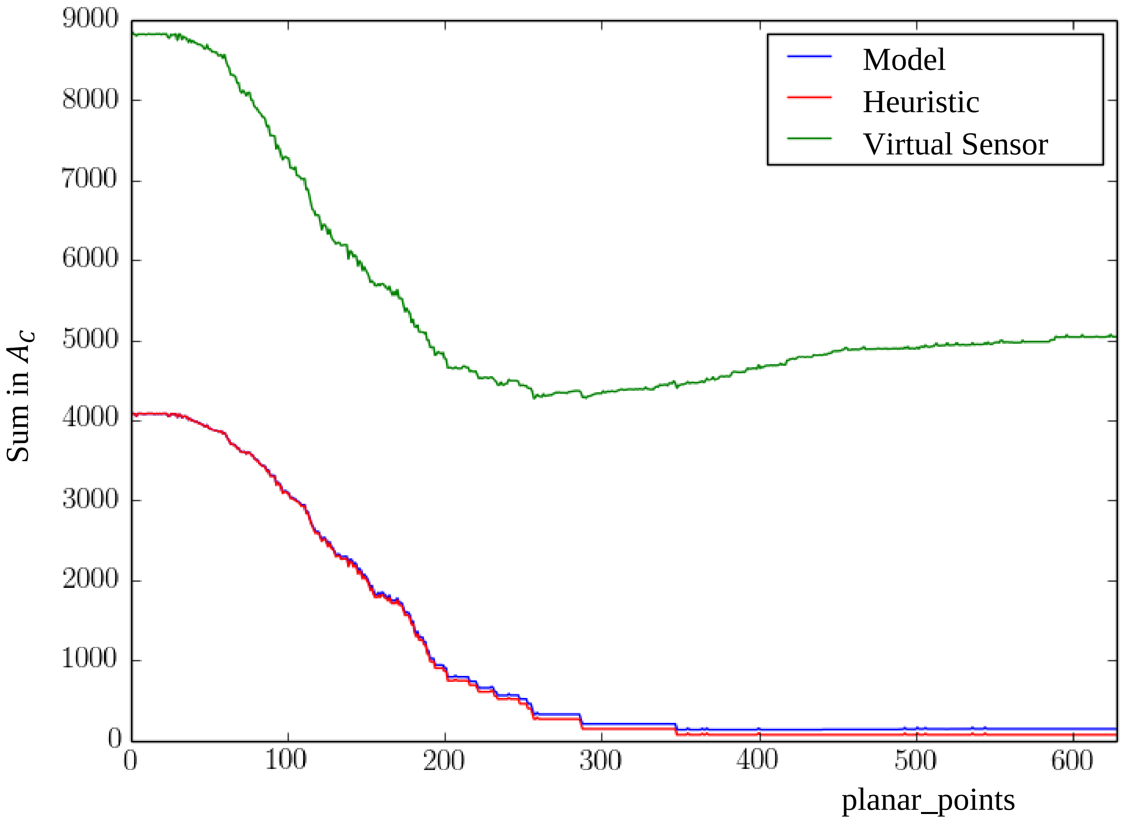

Fig. 19 Number of detected aerosol particles in **/fused_scan_2D** versus planar_points parameter

The total amount of detected aerosol particles from the virtual 2D LiDAR scan $S_{LiDAR,virtual\ 2D}$ (**/laser_scan_with_ransac**) is 5120. This shows that the virtual 2D scan already reduces the Type I effect. The recommended parameter setting is planar_points = 100, when using **/fused_scan_slam,** which can be seen in Fig. 20.

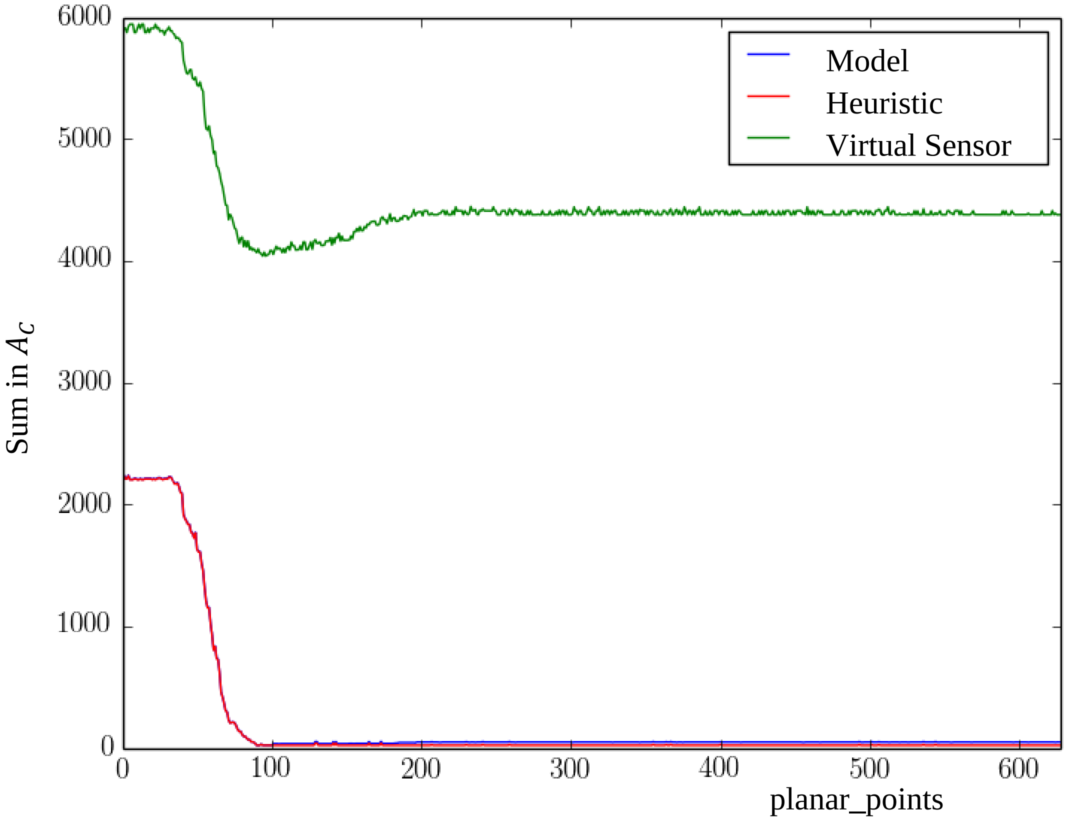

Fig. 20 Number of detected aerosol particles in **/fused_scan_slam** versus planar_points parameter

4.3 Experiments involving the Type II Effect

The Type II Effect occurs in environments with very dense smoke. The experimental set-up represents a search and rescue scenario involving smoke, where a robot is sent in, to create a map including the distribution of the smoke. Our scenario includes a small and a large room.

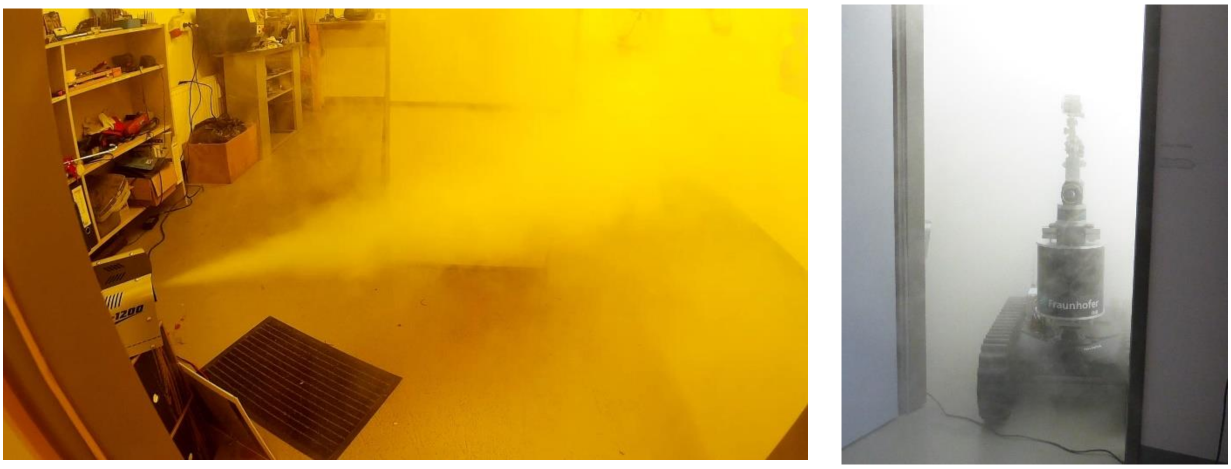

Fig. 21 In order to test the sensor fusion's capability to handle the Type II effect, we filled a room with very dense fog.

We filled the small room completely with fog, which can be seen behind the robot in Fig. 21. We observed that the LiDAR scan contains more invalide measurements, the more dense the fog. Although there was no suitable vision from RGB cameras inside the fog-room, it was possible to navigate the robot via the fused scans through the room. The scan fusion works very robustly and can be the input for mapping, localization and navigation algorithms. It combines the advantage of radar and LiDAR sensors as well as enhances the quality of mapping and localization. As we demonstrated in [3], maps which are built by the MPR, contain many outliers. On the other side, a LiDAR scanner's mapping result decreases as well in dense aerosol clouds. In environments without any aerosol, the resulting map from the fused scan S_{Fusion} is close as possible to a map, which is built only by LiDAR scans. The percentage of pure LiDAR, radar and fused scanpoint inside the fused scan in the moment the robot enters the foggy room is demonstrated in Fig. 22.

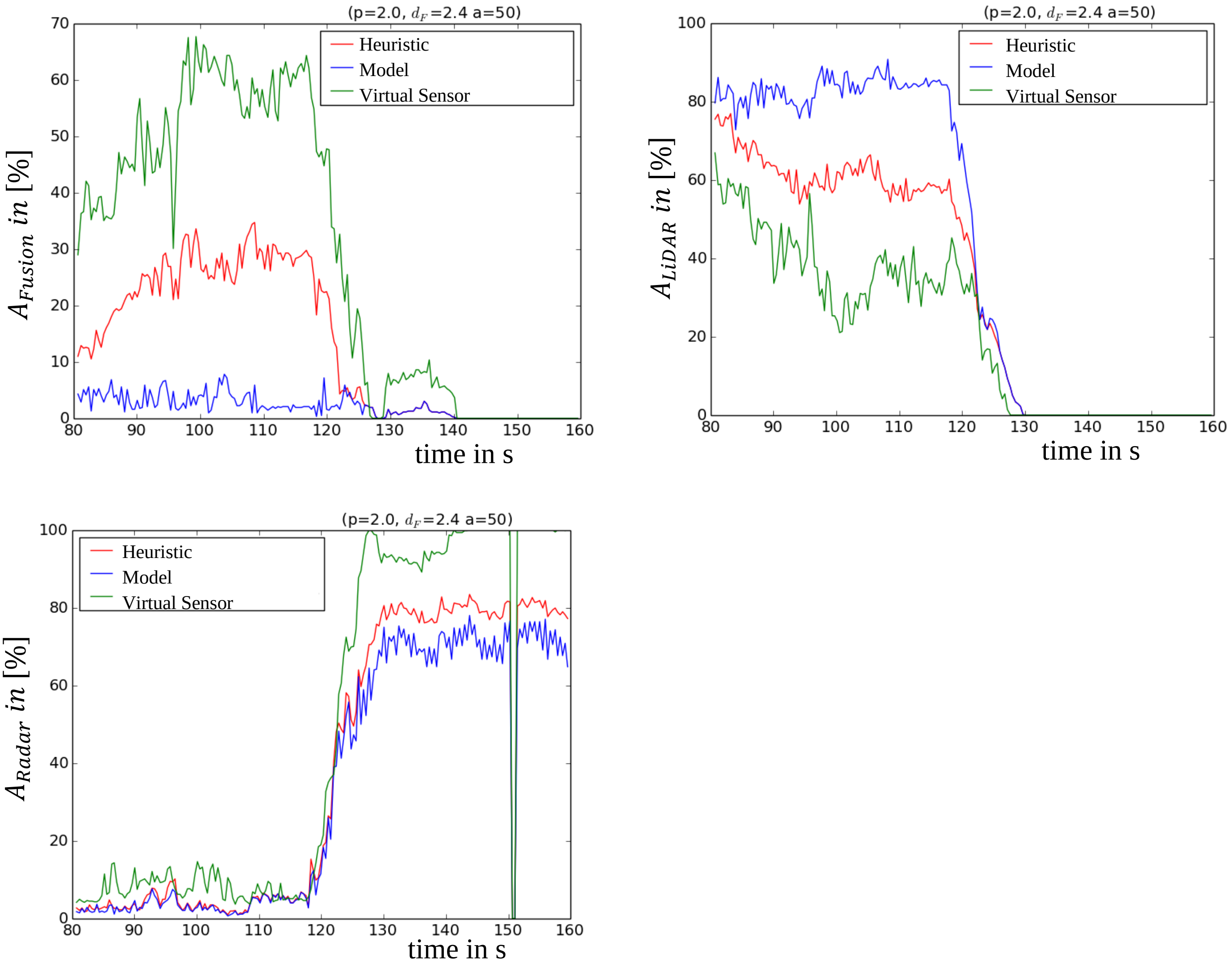

Fig. 22 Outside the foggy room, the percentage of LiDAR or fused scans is high. All three fusion approaches lead to only radar measurements inside the fused scan if the Type II effect occurs.

References

[1] Phillips, Tyson G. ; Guenther, Nicky ; McAree, Peter R.: When the Dust Settles: The Four Behaviors of LiDAR in the Presence of Fine Airborne Particulates. In: Journal of Field Robotics (2017)

[2] R. Brooks and S. Iyengar, Multi-sensor Fusion: Fundamentals and Applications with Software. Prentice Hall PTR, 1998.

[3] P. Fritsche, S. Kueppers, G. Briese, and B. Wagner, "Radar and LiDAR sensorfusion in low visibility environments," in Proc. 13th Int. Conf. Informatics, Automation and Robotics, vol. 2. Scitepress, 2016, pp. 30–36.

[4] O. Wulf, K. O. Arras, H. I. Christensen, and B. Wagner, "2D mapping of cluttered indoor environments by means of 3D perception," in Proc. Int. Conf. Robotics and Automation, vol. 4, 2004, pp. 4204–4209.